

Spinodal Decomposition and Nucleation in the Presence of Flow¹

A. Onuki²

Spinodal decomposition and nucleation of critical fluids are discussed in the presence of laminar shear and turbulence on the basis of recent experiments. In such situations we can realize stationary emulsion-like domain structures due to dynamical balance between thermodynamic instability and shear-induced deformations. In the spinodal decomposition case, unique is the strong shear regime in which the shear exceeds the average relaxation rate of the order parameter. In the nucleation case shear can enhance aggregation of droplets, thus speeding up the growth. But if the shear exceeds a relatively small critical value, even critical droplets can be broken, then leading to complete suppression of the droplet formation. We also predict a considerable increase of the effective viscosity and a large non-Newtonian effect due to domains in the course of spinodal decomposition.

KEY WORDS: fluid binary mixtures; light scattering; nucleation; shear flow; spinodal decomposition; viscosity.

1. INTRODUCTION

Fluid binary mixtures near the critical point are very suitable systems to investigate a variety of nonequilibrium effects both experimentally and theoretically. In equilibrium we find strong fluctuations in composition characterized by a semimacroscopic correlation length ξ and a semi-macroscopic average lifetime $t_\xi = \xi^2/D\xi$ ($\propto \xi^3$ in fluids). As a result the near-equilibrium behavior can be described on approaching the critical point in universal manners independently of details of fluids [1, 2]. On the other hand, there can be a number of nontrivial, nonequilibrium situations realizable in critical fluids, although well-studied examples are still limited.

¹ Invited paper presented at the Tenth Symposium on Thermophysical Properties, June 20–23, 1988, Gaithersburg, Maryland, U.S.A.

² Research Institute for Fundamental Physics, Kyoto University, Kyoto 606, Japan.

Most of such previous papers have been directed to the phase separation phenomena proceeding either by spinodal decomposition or by nucleation [3–7]. If a binary mixture is quenched at the critical composition $c = c_c$ into the unstable region $T < T_c$, the spinodal decomposition occurs and the characteristic size $R(t)$ of emerging domains evolves as $R(t) \sim t^\phi$, where t is the time after quenching. In an early stage $\phi \sim \frac{1}{3}$ (diffusion regime) and then $\phi \sim 1$ for $t \gtrsim 100t_\xi$ (capillary regime) as adequately explained by theories [6, 7]. However, there still remain many interesting open problems even here if the viewpoint is shifted. (i) No sufficient understanding has been obtained for the coarsening in a very late stage which starts with the onset of a gravity-induced convection (gravity regime) despite some remarkable observations [8]. (ii) Furukawa also examined another type of a very late stage in which domain sizes are so large that Reynolds numbers within characteristic domains exceed 1 and inertia effects are important (inertia regime) [9]. It should be relevant to density-matched fluid mixtures [10] and fluids not close to the critical point. (iii) We should also mention a very intriguing phase transition in a fluid mixture periodically driven through its critical point [11]. In experiments $\varepsilon \equiv T - T_c(p)$ was oscillated around an average $\langle \varepsilon \rangle$ by changing the pressure in a step-wise manner [12]. If $\langle \varepsilon \rangle$ was larger than a critical value ε_c (which was found to be positive), no macroscopic phase separation occurred and the system remained in a disordered phase state however long the observation time was. There, the scattered light intensity I_k behaved as $k^{-2.5}$ and was nearly stationary within each period at small wave numbers. In this disordered state, fluctuations are stronger than if the system were in equilibrium and at the critical point. It should also be remarked that the spatial correlation function has an anomalous long tail $r^{-0.5}$ at a large distance r . I believe that this disordered state deserves further scrutiny because of its unusual nature.³ On the other hand, for $\varepsilon < \varepsilon_c$, the phase separation proceeded, resulting in a macroscopic two-phase state, but it could be dramatically slowed down. Furthermore, as a surprising finding, the process depended on the control parameter $\varepsilon_c - \langle \varepsilon \rangle$ in a mean field fashion.

Another well-studied case is that of critical fluids in the one-phase region subjected to shear flow [14–16]. Here most of the critical fluctuations can be elongated along the flow before being dissipated thermally in the case $St_\xi \gtrsim 1$, S being the shear rate, as evidenced by anisotropic light

³ It would be exciting if we could make $T - T_c$ oscillate around zero by injecting relatively strong ultrasounds into systems near their second-order phase transition [13]. Then we could expect strong fluctuation enhancement due to periodic domain formation. This proposed experiment should be suitable even for systems with rapid time scales of the order parameter.

scattering [14]. Note that any spatial inhomogeneities are distorted by shear on the time scale of $1/S$ and this time can be easily made shorter than the thermal relaxation time t_ξ . Once we have $St_\xi \gtrsim 1$, the structure of the fluctuations is greatly different from that near equilibrium; the correlation range and the average lifetime are very anisotropic and no longer given by ξ and t_ξ , leading to unique nonequilibrium critical phenomena.

In this paper we focus our attention on effects of flow field (laminar shear flow or turbulence) on domains emerging in a phase-separating fluid brought into the unstable or metastable region. The effects are much more drastic than in the one-phase region. In Section 2 we examine spinodal decomposition in laminar shear, and in Section 3, spinodal decomposition in turbulence. Section 4 treats nucleation in flow. We are interested mainly in domain shapes and sizes in such flows, of which precise information can be obtained by light-scattering experiments. In Section 5 we consider a macroscopic rheological effect due to domains.

2. SPINODAL DECOMPOSITION IN LAMINAR SHEAR

2.1. Experiments So Far

Deformation and breakup of isolated droplets in laminar shear have long been studied in various (but noncritical) fluids since Taylor's pioneering work [17, 18]. In polymer physics, effects of shear on phase separation should be of prime importance, but such studies are still at a very premature level. Silberberg and Kuhn mixed two incompatible polymer pairs in a common solvent by applying shear to observe elongated domains [19]. With increasing shear, they eventually encountered disappearance of domain scattering and called it "phase separation reversal."

In a low molecular weight binary mixture quenched below T_c , Beysens and Perrot realized a periodic spinodal decomposition by periodically tilting a capillary tube through which the fluid passed [20]. A spinodal ring appeared when the tube was horizontal and the shear was small. Then it changed into a sharp streak as the tilting angle was increased. This arose from elongation of domains. Examples of the scattering patterns are shown in Fig. 1. The intensity was much stronger than that in the one-phase region.

Hashimoto's group has performed a shear flow experiment on a semi-dilute solution of polystyrene + polybutadiene + solvent [21]. They have found that, even if the fluid is initially in the two-phase state, the interface is broken in pieces and the fluid becomes homogeneous on application of stationary shear. At high shear they have observed a stationary sharp

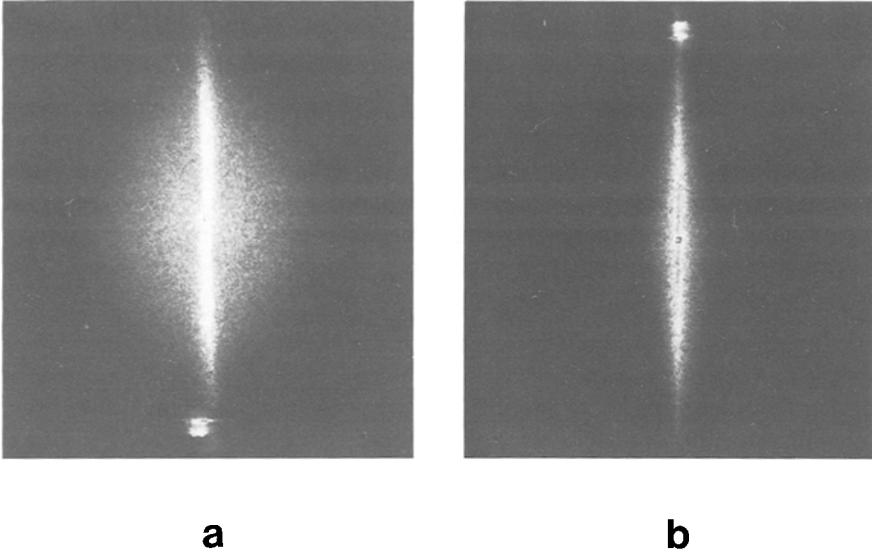


Fig. 1. Scattering patterns from a binary mixture of nitrobenzene + *n*-hexane at the critical composition below T_c by 3 mK [20]. Periodic shear is applied with the maximum 600 s^{-1} and the tilting frequency 0.317 s^{-1} and flow is nearly horizontal. (a) At an instant of $S=0$. (b) $S \neq 0$.

streak similar to the transient streak found by Beysens and Perrot. This result suggests that shear can stop the decomposition process, giving rise to anisotropic domain structures which are dynamically stationary as a result of the balance of the thermodynamic instability and the breakup mechanism by shear. Furthermore, they have studied shear-induced homogenization (the phase separation reversal in Silberberg's sense).

Very recently, Chan *et al.* have studied spinodal decomposition under stationary shear in the low molecular weight case [22]. As their first work they have followed deformation of the spinodal ring under weak shear to find results similar to those of the polymer case [21]. However, some aspects seem to be essentially different. One of them is the role of the hydrodynamic interaction in the two cases. In the low molecular weight case, small-scale velocity fluctuations induced by concentration inhomogeneities give rise to the renormalization of the diffusion constant [6] and the breakup and coagulation of domains [7]. In the polymer case, on the contrary, small-scale velocity fluctuations are strongly suppressed due to high viscosities [23]. As another difference, polymer systems show elastic behavior when polymer chains are deformed.⁴ However, because the

⁴ In polymer-solvent systems the elastic effects are much enhanced in the semidilute region, where a large shear-demixing effect was observed [24]. A theory for such effects will appear elsewhere.

study in the polymer case is still at the beginning, we consider only the low molecular weight case in the following [25, 26].

2.2. Weak Shear Case: Hydrodynamic Regime

We assume that the temperature T is slightly below the critical value T_c and the composition is at the critical value. Then there are two characteristic cases, $St_\xi < 1$ and $St_\xi > 1$. Here $t_\xi \equiv 6\pi\eta\xi^3/k_B T$ is the characteristic time scale of the critical fluctuations, η being the shear viscosity and $\xi = \xi_0(1 - T/T_c)^{-\nu}$ being the correlation length. In Fig. 2 we show schematically domain structures in these two cases in b and c, while in a the gravity effect is dominant and the interface is not broken.

First let us consider the steady state in the very weak shear case $St_\xi \ll 1$. Domains will have sizes much greater than ξ and sharp interfaces. Let R_\perp and R_\parallel be the characteristic domain sizes perpendicular and parallel to the flow. The gravity effect will be negligible if R_\parallel is less than the capillary length $(\sigma/g\Delta\rho)^{1/2}$, where σ is the surface tension and $\Delta\rho$ is the

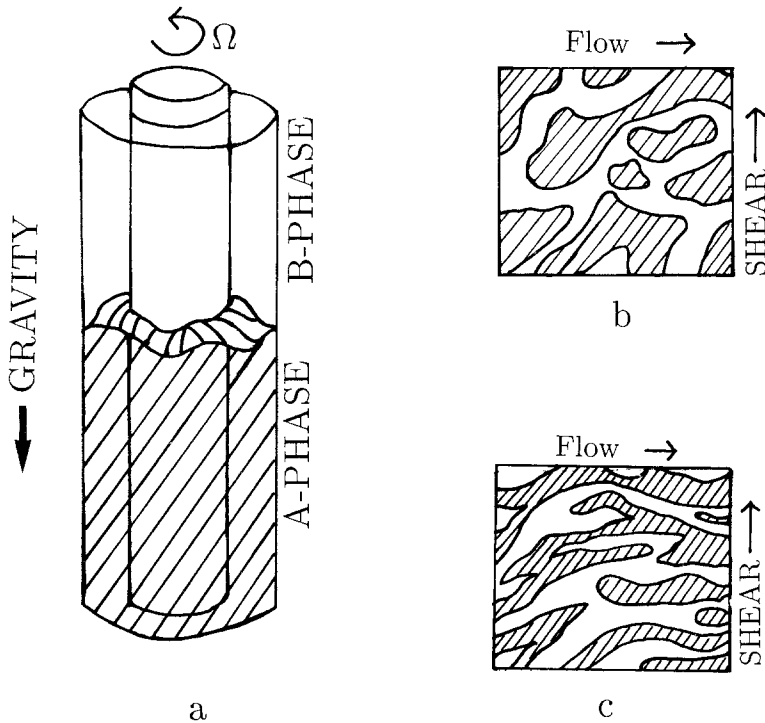


Fig. 2. Schematic domain structures of fluids in the two-phase region under gravity and shear flow. Shear is produced by a concentric rotating cylinder. (a) Gravity-dominated case. (b) Weak shear case. (c) Strong shear case.

mass-density difference between the two phases. The interface velocity is equal to the velocity field $\mathbf{u}(\mathbf{r}, t)$ at the interface position. Here $\mathbf{u}(\mathbf{r}, t)$ obeys the usual Navier–Stokes equation where the pressure is discontinuous across the interface by $\sigma\kappa$, κ being the curvature. Neglecting the effect of inertia, we find [18]

$$\mathbf{u}(\mathbf{r}) \cong Sy\mathbf{e}_x + \left[\frac{\sigma}{\eta} \right] \int da' \vec{T}(\mathbf{r} - \mathbf{r}') \cdot \mathbf{n}(\mathbf{r}') \kappa(\mathbf{r}') \quad (1)$$

where the first term is the average flow, \mathbf{e}_x being the unit vector along the x axis, $\int da'$ is the surface integral over the interface position \mathbf{r}' , $\mathbf{n}(\mathbf{r}')$ is the normal unit vector at the interface, and $\vec{T}(\mathbf{r})$ is the Oseen tensor ($\propto 1/r$). The competition of the two terms in Eq. (1) should result in a stationary state. Hence, simple dimension analysis yields

$$R_{\perp} \sim R_{\parallel} \sim \sigma/\eta S \quad (2)$$

However, Chan et al. have found a sharp streak even for $St_{\xi} \sim 1$ [22]. This suggests that in the percolated case at the critical composition R_{\parallel} can be considerably greater than R_{\perp} even for $St_{\xi} \sim 1$, in contrast to the isolated droplet case [17, 18]. This point should be examined further in the future.

On the basis of Eq. (2) the inertia term is estimated as $\rho(\mathbf{u} \cdot \nabla) \mathbf{u} \sim (\rho\sigma^2/\eta^3 S)(\eta\nabla^2 \mathbf{u})$. Thus the Reynolds number R_e is of order $\rho\sigma^2/\eta^3 S$ and Eq. (2) is valid only in the low-Reynolds number case,

$$S > \rho\sigma^2/\eta^3 \quad \text{or} \quad St_{\xi} > \rho\sigma\xi/\eta^2 \quad (3)$$

As $T \rightarrow T_c$, we have $(\sigma/g \Delta\rho)^{1/2} \ll \eta^2/\rho\sigma$ except for density-matched fluid mixtures [10]. Then the effect of inertia can be neglected (before the gravity effect becomes dominant), and Eq. (2) holds in the following shear region:

$$1/\tau_{\xi} \gg S > (\sigma g \Delta\rho)^{1/2}/\eta \quad (4)$$

We call this regime the capillary regime in shear. Notice the close analogy of Eq. (2) and the growth law $R(t) \sim (\sigma/\eta)t$ in the capillary regime in the normal spinodal decomposition case. For $k \lesssim 1/R_{\parallel}$ the scattered light intensity will be of the order given by $I_k \sim (\Delta c)^2 R_{\parallel} R_{\perp}^2 \sim (T_c - T)^{2\beta} (\sigma/\eta S)^3$, where Δc is the concentration difference. On the other hand, in the gravity regime $S < (\sigma g \Delta\rho)^{1/2}/\eta$, the fluid will tend to a macroscopic two-phase state, although its details are unknown.

At this point we should not overlook that many systems satisfy the reverse condition $(\sigma/g \Delta\rho)^{1/2} \gg \eta^2/\rho\sigma$ far from T_c . For such cases there is a shear region in which $R_e > 1$ and the gravity effect is negligible. Here

$R \sim (\sigma/\rho S^2)^{1/3}$ by equating the capillary pressure σ/R and the dynamic pressure $\rho(SR)^2$. The corresponding shear region is written as

$$\rho^{-1/2} \sigma^{-1/4} (g \Delta \rho)^{3/4} < S < \rho \sigma^2 / \eta^3 \quad (5)$$

This regime may be called the inertia regime in shear [9, 26].

2.3. Strong Shear Case: Nonhydrodynamic Regime

The case $St_\xi > 1$ can be realized only in critical fluids and it can be rewritten at the critical composition as

$$|T - T_c|/T_c < \bar{\tau}_s = (6\pi\eta_0 \xi_0^3 S/k_B T)^{1/(3\nu)} \quad (6)$$

For example, $\bar{\tau}_s \simeq 10^{-5} S^{0.53}$ (S in s^{-1}) for isobutyric acid + water, while it is much smaller for pure fluids as exemplified by $\bar{\tau}_s \simeq 6 \times 10^{-7} S^{0.53}$ for xenon. Then we introduce a wave number k_c by

$$(k_B T/6\pi\eta) k_c^3 = S \quad \text{or} \quad k_c \xi = (S\tau_\xi)^{1/3} \quad (7)$$

The fluctuations with wave numbers greater than k_c are denoted by SWF, and those with wave numbers smaller than k_c by LWF. The LWF are strongly elongated along the flow and their lifetime and the correlation length are no longer given by τ_ξ and ξ , while SWF are little affected by shear. A renormalization group theory [15] showed that a mean field theory can be used once SWF have been coarse-grained in the theory. The LWF are suppressed below the equilibrium level such that the nonlinear coupling among LWF can be taken into account by a normal perturbation scheme in three dimensions.

In the disordered phase the fluctuation intensity $I_k = \langle |c_k|^2 \rangle$ for LWF is roughly described by

$$I_k \sim 1/\{A[T - T_c(S)] + ck_c^{8/5} |k_x|^{2/5} + k^2\} \quad (8)$$

where $A = \xi_0^{-2} (\bar{\tau}_s)^{2\nu-1} / T_c$ and $c \sim 1$. In Ref. 15 the critical temperature $T_c(S)$ was found to be slightly lower than the equilibrium value $T_c(0)$. There, the shift $\Delta T = T_c(0) - T_c(S)$ was calculated in the $\epsilon = 4 - d$ expansion scheme (where d is the spatial dimensionality):

$$\Delta T = T_c(0) - T_c(S) = [0.0832\epsilon + O(\epsilon^2)] \bar{\tau}_s T_c(0) \quad (9)$$

At $d = 3$ we expect $\Delta T/T_c \sim \frac{1}{10} \bar{\tau}_s$ from the experiments [14].

On the other hand, if T is lowered below $T_c(S)$ under Eq. (6), the spinodal decomposition occurs leading to the anisotropic domain structure

shown in Fig. 2c. Equation (8) suggests that the spatial scale perpendicular to the flow ($k_x \cong 0$) should initially be given by $1/\kappa$ with

$$\kappa = \xi_0^{-1} (\bar{\tau}_s)^{\nu-1/2} [(T_c(S) - T)/T_c]^{1/2} \quad (10)$$

In Ref. 26 I expected that the domain size R_{\perp} perpendicular to the flow in the final steady state does not much exceed $1/\kappa$, so that

$$R_{\perp} \sim 1/\kappa \quad (11)$$

Next, assuming that domains are elongated for a time t_c before their breakup on the average, we have $R_{\parallel} \sim St_c/\kappa$. In Ref. 26, on the basis of a perturbation calculation in Ref. 25, t_c was estimated as $6 \ln(k_c/\kappa)/\Gamma_{\perp}$, where $\Gamma_{\perp} \sim (k_B T/6\pi\eta k_c) \kappa^4$ is the inverse time scale of the fluctuations⁵ homogeneous along the flow ($k_x = 0$) and varying in the perpendicular directions on the scale of $1/\kappa$. To make only crude estimates we neglect the logarithmic factor in t_c to obtain a domain size parallel to the flow,

$$R_{\parallel} \sim k_c^4/\kappa^5 \propto S^{1.0} [T_c(S) - T]^{-2.5} \quad (12)$$

The elongation ratio is given by

$$R_{\parallel}/R_{\perp} \sim (k_c/\kappa)^4 \propto S^{2/(3\nu)} [T_c(S) - T]^{-2} \quad (13)$$

We must say that the relation $t_c \propto 1/\Gamma_{\perp}$ is still a conjecture.

To explain the streak in Fig. 1, we next consider the scattered light intensity, which should be of the following anisotropic form $I_k \sim \langle (\Delta c)^2 \rangle R_{\parallel} R_{\perp}^2 f(R_{\parallel} k_x, R_{\perp} k_y, R_{\perp} k_z)$, where $f(x, y, z)$ is a scaling function and $\langle (\Delta c)^2 \rangle$ is the average of the square of the concentration deviation at a point. In this paper we can assert only

$$\langle (\Delta c)^2 \rangle \lesssim \text{const.} (\bar{\tau}_s)^{2\beta-1} (T_c(S) - T) \quad (14)$$

The right-hand side of Eq. (14) would be the square of the concentration difference if a planar macroscopic interface parallel to the flow would separate the two phases. The equality in Eq. (14) might not hold in view of the fact that the domain size R_{\perp} perpendicular to the flow does not much exceed the interfacial width $1/\kappa$ in the steady state.

It should be noted that Eq. (14) does lead to phase separation reversal in the low molecular weight case even in this form.⁶ It occurs when $T = T_c(S) = T_c(0) - \Delta T$ or $St_{\xi} = [0.0832\varepsilon + \dots]^{-3\nu} \sim 100$, where use has been made of Eq. (9).

⁵ The kinetic coefficient (the diffusion constant multiplied by the concentration susceptibility) is proportional to $1/k_c$ in strong shear [14].

⁶ For example, the domain contribution to the turbidity vanishes as $T \rightarrow T_c(S)$.

3. TURBULENT CRITICAL BINARY MIXTURES

First we introduce Kolmogorov's theory for droplet sizes in turbulence [27–29]. We neglect gravity effects and the density difference between fluids inside and fluids outside droplets. Then there are two characteristic cases, $R > 1/k_d$ and $R < 1/k_d$, where $k_d = L_0^{-1} R_e^{3/4}$ is the Kolmogorov cutoff wave number, L_0 being the size of the largest eddies and R_e being the Reynolds number.

(i) In the inertial range $R > 1/k_d$, he obtained the characteristic size R by equating the capillary pressure σ/R and the difference of the dynamic pressures, Δp , exerted on opposite sides of droplets. His scaling theory of turbulence then shows $\Delta p \sim \rho u_R^2$, where $u_R = (\varepsilon_0 R)^{1/3}$ is the characteristic velocity of eddies with size R , ε_0 being the energy dissipation rate per unit mass. This is based on the picture that eddies with size R should deform the interface most dominantly. Thus,

$$R \sim (\sigma/\rho)^{3/5} \varepsilon_0^{-2/5} \sim (\rho\sigma/\eta^2)^{3/5} k_d^{-8/5} \quad (15)$$

(ii) In the dissipative range $R < 1/k_d$, however, he erroneously obtained $R \sim (\rho\sigma/\eta^2)^{1/3} k_d^{-4/3}$ from the balance $\sigma/R \sim \rho u_R^2$, with $u_R \sim S_d R$, $S_d = (\eta/\rho) k_d^2$ being the typical shear rate in the dissipative range. It should be noted that the Reynolds number associated with such a small droplet is smaller than 1 from $R(RS_d)/(\eta/\rho) \sim (k_d R)^2 \ll 1$. Then, σ/R must be balanced with the shear stress ηS_d , so that

$$R \sim \sigma/\eta S_d \quad (16)$$

The two equations, (15) and (16), are continuously connected at $R \sim 1/k_d$, which holds for $\sigma \sim (\eta^2/\rho) k_d$. We have Eq. (16) for $\sigma < (\eta^2/\rho) k_d$, which is eventually satisfied near the critical point since $\sigma \propto (T_c - T)^{2\nu}$. We may call the case of Eq. (16) the capillary regime in turbulence.

For critical binary mixtures Ruiz and Nelson [30] first studied transient mixing processes, although the predicted effect was not supported by a subsequent experiment [31]. Afterward, experiments in Pittsburgh have been focused on light scattering from continuously stirred critical binary mixtures at the critical composition [32, 33]. In such a case stirring suppresses the growth of domains, resulting in a dynamical stationary state as in the laminar shear case.

The picture of the phenomena is as follows [34]. The characteristic concentration fluctuations have sizes smaller than that of the smallest eddies ($\sim 1/k_d$) and they are strained by random shear which may be regarded as spatially homogeneous. The straining is most effectively caused by the smallest eddies with shear $S_d = (\eta/\rho) k_d^2$. The turnover time of these

eddies is of the order $t_d = 1/S_d$ and this time is also the duration time during which the concentration fluctuations are acted by the eddies.

On the basis of this picture, Ref. 34 used an approximation scheme devised by Kraichnan, who developed a theory for the diffusion of a passive scalar quantity in the dissipative range [35]. To calculate the two-point correlation function $I_k(t) = \langle |c_k(t)|^2 \rangle$, he approximated the velocity gradient tensor $\{\partial u_i / \partial x_j\}$ as a white noise independent of space. Then $I_k(t)$ obeys

$$\frac{\partial}{\partial t} I_k(t) = B \left[k^2 \frac{\partial^2}{\partial k^2} + 4k \frac{\partial}{\partial k} \right] I_k(t) + X_k(t) \tag{17}$$

where B is of the order S_d from Kolmogorov's scaling theory and $X_k(t) = -2Dk^2 I_k(t)$ in Kraichnan's case. In the case of unstable fluids $X_k(t)$ was set equal to the time derivative in Kawasaki and Ohta's equation [6], which takes into account the hydrodynamic interaction within Langer and co-workers' scheme [36].

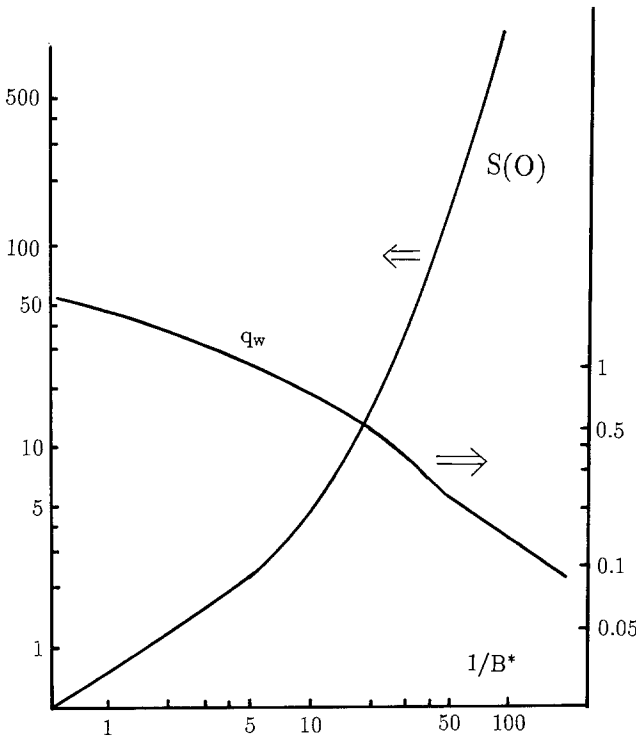


Fig. 3. The maximum $S(0) = \xi^2 I_0$ and the wave number $q_w = \xi k_w$ versus $1/B^*$ from the theory [34].

The theoretical results are as follows. As $t \rightarrow \infty$, $I_k(t)$ tends to a stationary intensity I_k , which has the following features.

(i) I_k is peaked at $k=0$ (no spinodal ring). In Fig. 3 the dimensionless intensity $S(0) = \xi^{-2} I_0$ for $k \rightarrow 0$ is shown as a function of the inverse of a dimensionless shear defined by

$$B^* = t_\xi B \sim (6\pi\eta\xi^3/k_B T) S_d \quad (18)$$

(ii) We also plot the dimensionless width $q_w = \xi k_w$ versus $1/B^*$, where k_w is defined by $I_{k_w} = \frac{1}{2} I_0$. The behavior is very analogous to that of the dimensionless peak wave number $q_m = \xi k_m$ versus $\tau = t/t_\xi$ in the normal spinodal decomposition process [3, 4]. Our model given by Eq. (17) thus indicates that the spinodal decomposition is stopped at a time of the order $t_\xi/B^* \sim 1/S_d$. The effective exponent $\phi = d(\ln q_m)/d(\ln B^*)$ changes from $\frac{1}{3}$ to 0.7 with increasing $1/B^*$. However, the capillary regime, in which $q_w \sim B^*$ [see Eq. (16)], cannot be reached as long as our scheme is based on Kawasaki and Ohta's approximation.⁷ We naturally expect that our scheme is applicable only for $1/B^* \lesssim 100$ and the crossover to the capillary regime should occur for $1/B^* \gtrsim 100$.

⁷ Their theory does not take into account the breakup mechanism of domains.

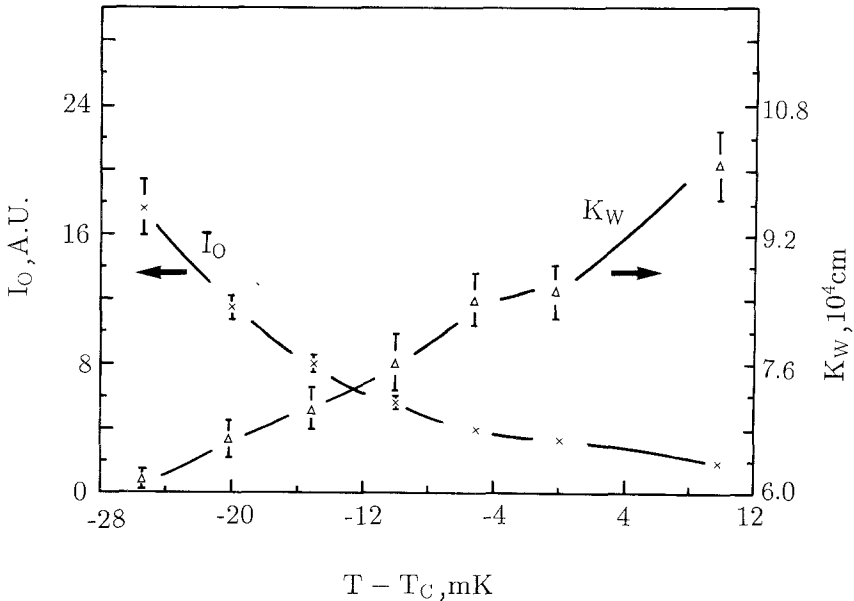


Fig. 4. The scattered light intensity in the limit $k \rightarrow 0$ and the wave number k_w versus $T - T_c$ for isobutyric acid + water stirred at 14.2 Hz, which corresponds to $Re \sim 10^4$.

Next we show data in Ref. 33. In Fig. 4 experimental values for $I_0 = \xi^2(0)$ and $k_w = \xi^{-1}q_w$ are displayed as functions of $T - T_c$. To interpret the data within our theoretical scheme let us set $q_w \sim (B^*)^\phi$ to obtain $k_w \sim S_d^\phi(T_c - T)^{(1-3\phi)\nu}$. For instance, at $T_c - T = 20$ mK, Fig. 4 shows $d(\ln k_w)/d[\ln(T_c - T)] \sim -0.5$, which then suggests $\phi \sim 0.6$ from Eq. (19). Obviously in the experiment the quench depth was not so deep and the capillary regime was not reached. In Fig. 5 the scaled intensity $F(k/k_w) = I_k/I_0$ is shown for some temperatures. The agreement with the theoretical curve at $B^* = 0.1$ is remarkable.⁸

The theory of Ref. 34 and also the experiment suggest that there is no sharp phase transition under stirring, while some authors expected a critical point [37]. In the laminar shear case, on the contrary, the intensity in the disordered phase given by Eq. (8) shows that a critical point $T = T_c(S)$ still exists, although the critical divergence is much weakened due to the term proportional to $|k_x|^{2/5}$ in I_k .

⁸ The scaling function $F(x)$ still depends on B^* in our model, although the dependence is rather weak.

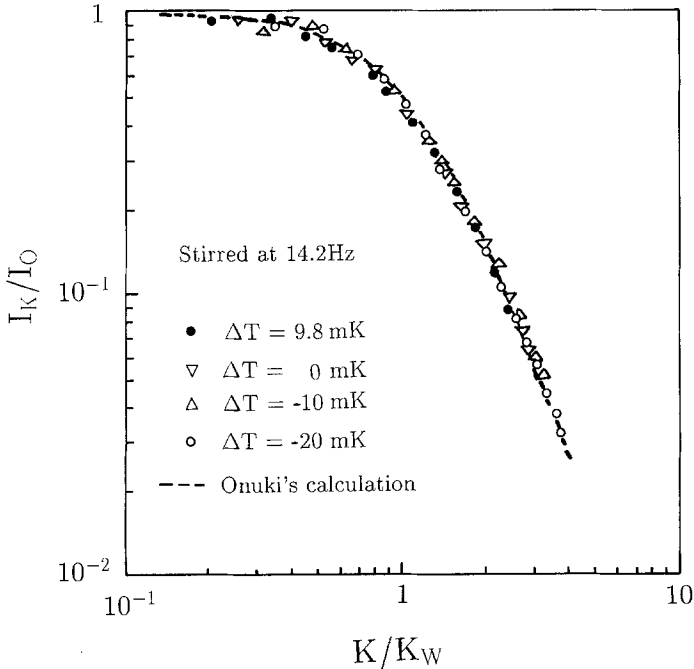


Fig. 5. $F(k/k_w) = I_k/I_0$ versus k/k_w on a log-log scale. The dashed curve is the theoretical curve at $B^* = 0.1$.

4. NUCLEATION IN FLOW WITH WEAK SHEAR

Let us supercool a fluid mixture at the off-critical condition in the presence of flow field. Droplets must be torn when the capillary pressure ($\sim \sigma/R$) is much less than the shear stress ηS [17, 18]. This results in an upper limit of the droplet size, $R^* \sim \sigma/\eta S$. Noticeable droplets can emerge only when the critical radius $r_c (\sim \xi/\phi)$ is smaller than R^* , ϕ being the volume fraction much less than 1. This condition is rewritten as $St_\xi < \phi \ll 1$. Our arguments are applicable also to stirred fluids if S is replaced by the maximum shear S_d .

Another interesting aspect is that droplets coagulate in shear flow. Let us assume an initial distribution of an appreciable number of droplets greater than r_c . To a droplet with the typical radius R , nuR^2 droplets are approaching per unit time by the relative convective motion, where $n \sim \phi/R^3$ is the droplet density and $u \sim SR$ is the relative velocity. Thus, n decreases by the coagulation as

$$\left(\frac{\partial}{\partial t} n\right)_c \sim -(nuR^2) n \sim -S\phi n \quad (19)$$

Therefore the droplet density (or size) will decrease (or increase) exponentially with a rate of the order $S\phi$. The saturation will then occur for $R \sim R^*$, where there will be a dynamical balance between the breakup and the coagulation. The evolution of the droplet distribution can be studied more precisely by setting up a Smoluchowski equation [38, 39, 29]. The final droplet distribution will be sharply peaked at $R = R^*$. On the other hand, in the usual case without shear, anomalous supercooling has been observed as $T \rightarrow T_c$ [4, 5]. Namely, emergence of appreciable droplets can be very slow as $T \rightarrow T_c$ even if $(T_{CX} - T)/(T_c - T_{CX})$ much exceeds the classical cloud point value of order 0.15, where T_{CX} is the temperature on the coexistence curve for a given concentration. Interestingly, in the presence of flow, the flow-induced aggregation eventually dominates over the diffusion or Lifshitz-Slyozov process even for very low shear in a time of the order $1/S\phi$. It is worth trying to observe competition of these two mechanisms at very low shear.

It is also of interest to investigate how shear can affect the birth process of critical droplets [4]. If such an effect exists, the cloud point itself will become dependent on the shear. However, no definite conclusion can be made on this aspect at present because of the lack of detailed information how localized thermal fluctuations without distinct contrast between the two phases grow up to a critical droplet with a sharp interface.

In the case of laminar shear light scattering can also give information on anisotropic shapes of droplets, which are expected to be nearly

spheroids [17 18]. In the case of stirring there is no preferred direction and scattering is isotropic, but droplets should be strongly distorted from spheres.

5. PROPOSAL OF CRITICAL RHEOLOGY

In Ref. 40 the shear viscosity was predicted to increase considerably due to domains in critical fluids quenched into the unstable or metastable region. This effect should be detectable if the viscosity measurement is carried out in the course of spinodal decomposition before the system is macroscopically phase-separated. Let us consider a torsionally oscillating cylinder. Spinodal decomposition under shear should occur in a boundary layer with thickness $(2\eta/\rho\omega)^{1/2}$ next to the cylinder wall. Here our results in Section 3 can be used if the oscillating frequency ω is much less than the typical shear S in the layer. Domains near the critical point are so easily broken into small fragments that the domain structure in the layer should be kept independent of the time after quenching. We consider the excess viscosity $\Delta\eta$ in the low-frequency limit $\omega \ll S$ in the following limiting cases.

(i) In the capillary regime, given by Eqs. (3) and (4), the characteristic domain size is given by $R \sim \sigma/\eta S$. Since domains are continuously elongated, a surface energy of order σR^2 is supplied to each domain from the outside on the time scale of $1/S$. This energy is eventually dissipated into heat at breakup, the dissipation time being $R^2/(\eta/\rho) \sim R_e/S < 1/S$. The resultant extra dissipation gives rise to a viscosity increase $\Delta\eta$ determined by $(\Delta\eta) S^2 \sim (\phi\sigma/R) S$, where $\phi\sigma/R$ is the surface energy density, ϕ being the volume fraction. Thus,

$$\Delta\eta/\eta \sim \phi \quad (20)$$

where η is the viscosity in the absence of domains (that in the one-phase state with the same $T_c - T$). This relation is well-known for dilute systems of emulsions. However, in our case domains are nonlinearly deformed, whereas in usual emulsion systems Eq. (20) holds only for infinitesimal deformations. (ii) In the inertia regime given by Eq. (5) we limit ourselves to $\phi = \frac{1}{2}$. Since the characteristic velocity fluctuation is of the order $SR \sim (\sigma S/\rho)^{1/3}$, we find

$$\Delta\eta/\eta \sim Re \sim (\rho\sigma^2/\eta^3 S)^{1/3} \gtrsim 1 \quad (21)$$

(iii) In the the strong shear case $\Delta\eta$ should rapidly decrease as domains are elongated and the contrast between the two phases becomes

ill defined. In Ref. 40, assuming the equality in Eq. (14), we predicted the following non-Newtonian effect:

$$\Delta\eta/\eta \sim \phi(St_\xi)^{-4/3\nu} \quad (22)$$

On the other hand, if $\omega \gtrsim S$, $\Delta\eta$ should strongly depend on ω even when $\omega t_\xi \ll 1$. A large normal stress effect can also be expected in the presence of domains [40].

6. CONCLUDING REMARKS

The topics in this paper may be claimed to constitute one of actively evolving fields in nonequilibrium statistical physics. Our consideration should be extended to more complex fluid systems with domain structures such as microemulsions, liquid crystals, entangled polymers, block copolymers, etc.

REFERENCES

1. J. V. Sengers and J. M. H. Levelt Sengers, in *Progress in Liquid Physics*, C. A. Croxton, ed. (Wiley, Chichester, England, 1978), pp. 103–174.
2. K. Kawasaki and J. D. Gunton, in *Progress in Liquid Physics*, C. A. Croxton, ed. (Wiley, Chichester, England, 1978), pp. 175–211.
3. N. C. Wong and C. K. Knobler, *J. Chem. Phys.* **69**:725 (1978); Y. C. Chou and W. I. Goldburg, *Phys. Rev. A* **20**:2105 (1979).
4. W. I. Goldburg, in *Light Scattering Near the Phase Transition*, H. Z. Cummins and A. P. Levanyuk, eds. (North-Holland, Amsterdam), pp. 531–581, and references therein.
5. K. Binder and D. Stauffer, *Adv. Phys.* **25**:343 (1976); J. S. Langer and A. J. Schwartz, *Phys. Rev. A* **8**:948 (1980).
6. K. Kawasaki and T. Ohta, *Prog. Theor. Phys.* **59**:362 (1978).
7. E. D. Siggia, *Phys. Rev. A* **20**:595 (1979).
8. C. K. Chan and W. I. Goldburg, *Phys. Rev. Lett.* **58**:674 (1987).
9. H. Furukawa, *Phys. Rev. A* **31**:3857 (1985).
10. C. Houessou, P. Guenoun, R. Gastaud, F. Perrot, and D. Beysens, *Phys. Rev. A* **32**:1818 (1985).
11. A. Onuki, *Prog. Theor. Phys.* **67**:1740 (1982); *Phys. Rev. Lett.* **48**:753 (1982).
12. M. Joshua, J. V. Maher, and W. I. Goldburg, *Phys. Rev. Lett.* **51**:196 (1983); M. Joshua, W. I. Goldburg, and A. Onuki, *Phys. Rev. Lett.* **54**:1175 (1985); M. Joshua and W. I. Goldburg, *Phys. Rev. A* **31**:3857 (1985).
13. A. Onuki, *Prog. Theor. Phys.* **66**:1230 (1981); *Prog. Theor. Phys.* **67**:768 (1982); *Prog. Theor. Phys.* **67**:787 (1982).
14. D. Beysens, M. Gbadamassi, and L. Boyer, *Phys. Rev. Lett.* **43**:1253 (1979); D. Beysens and M. Gbadamassi, *J. Phys.* **40**:L-565 (1979); *Phys. Rev. A* **22**:2250 (1980); D. Beysens, M. Gbadamassi, and B. Moncef-Bouonz, *Phys. Rev. A* **28**:2491 (1983).
15. A. Onuki and K. Kawasaki, *Prog. Theor. Phys. Suppl.* **64**:436 (1978); *Ann. Phys.* **121**:456 (1979); A. Onuki, K. Yamazaki, and K. Kawasaki, *Ann. Phys.* **131**:217 (1981).
16. A. Onuki, *Physica A* **140**:204 (1986).

17. G. I. Taylor, *Proc. Roy. Soc.* **A146**:501 (1934).
18. J. M. Rallison, *Annu. Rev. Fluid Mech.* **16**:145 (1984), and references therein.
19. A. Silberberg and W. Kuhn, *J. Polymer Sci.* **8**:21 (1954).
20. D. Beysens and F. Perrot, *J. Phys.* **45**:L-31 (1984).
21. T. Hashimoto, T. Takebe, and S. Suehiro, *J. Chem. Phys.* **88**:5874 (1988); *Polymer* **29**:227 (1988); *Polymer* **29**:261 (1988).
22. C. K. Chan, F. Perrot, and D. Beysens, *Phys. Rev. Lett.* **61**:412 (1988).
23. T. Hashimoto, in *Dynamics of Ordering Process in Condensed Matter*, S. Komula and H. Furukawa, eds. (Plenum, New York, 1988); A. Onuki, *J. Chem. Phys.* **85**:1122 (1986).
24. C. Rangel-Nafaile, A. B. Metzner, and K. F. Wissbrun, *Macromolecules* **17**:1187 (1984).
25. T. Imaeda, A. Onuki, and K. Kawasaki, *Prog. Theor. Phys.* **71**:16 (1984).
26. A. Onuki, *Phys. Rev.* **A34**:3528 (1986).
27. A. N. Kolmogorov, *Dokl. Akad. Nauk. SSSR* **66**:825 (1949).
28. V. G. Levich, *Physicochemical Hydrodynamics* (Prentice-Hall, Englewood Cliffs, N.J., 1962), Chap. 8.
29. A. Onuki and S. Takesue, *Phys. Lett.* **114A**:133 (1986).
30. R. Ruiz and D. R. Nelson, *Phys. Rev.* **A23**:3224 (1981); *Phys. Rev.* **A24**:2727 (1981).
31. N. Eswar, J. V. Maher, D. J. Pine, and W. I. Goldburg, *Phys. Rev. Lett.* **51**:1272 (1983); C. K. Chan, J. V. Maher, and W. I. Goldburg, *Phys. Rev.* **A32**:311 (1985).
32. D. J. Pine, N. Eswar, J. V. Maher, and W. I. Goldburg, *Phys. Rev.* **A29**:308 (1984).
33. C. K. Chan, W. I. Goldburg, and J. V. Maher, *Phys. Rev.* **A35**:1756 (1987).
34. A. Onuki, *Phys. Lett.* **A101**:286 (1984).
35. R. H. Kraichnan, *Phys. Fluids* **11**:945 (1968).
36. S. Langer, M. Bar-on, and H. D. Miller, *Phys. Rev.* **A11**:1417 (1975).
37. J. Aronovitz and D. R. Nelson, *Phys. Rev.* **A29**:2012 (1984); G. Satten and D. Ronis, *Phys. Rev.* **A33**:3415 (1986).
38. D. L. Swift and S. K. Friedlander, *J. Colloid Sci.* **19**:621 (1964).
39. P. G. Saffman and J. S. Turner, *J. Fluid Mech.* **1**:16 (1956).
40. A. Onuki, *Phys. Rev.* **A35**:5149 (1987).